2013

Quantifying Adhesion between Polyelectrolyte Multilayers

Walter A. Jokiel
Lehigh University

Quantifying Adhesion between Polyelectrolyte Multilayers

By

Walter A Jokiel

Thesis Presented to the Graduate and Research Committee of

Lehigh University

In Candidacy for the Degree of

Master of Science

In

Bioengineering

Lehigh University

January 2013

Certificate of Approval:

This thesis is accepted and approved in partial fulfillment of the requirements for the Master of Science.

Date:

Advisor Name:

Department Chair:

Acknowledgements:

This work was supported by the US Department of Energy, Office of Basic Energy Sciences, Division of Materials Sciences and Engineering under award DE-FG02-07ER46463.

We acknowledge the laboratory of Prof. Chaudhury of Lehigh University for their assistance in developing the technique of polyelectrolyte deposition, and thank Xun Gong of the Mayo Research Clinic's graduate program and William Lenthe of Lehigh University's Materials Science and Engineering department for their help.

Contents

Quantifying Adhesion between Polyelectrolyte Multilayers

Abstract:

The adhesion between poly(acrylic acid) (PAA) and poly(allylamine hydrochloride) (PAH) deposited on oxygen plasma-treated polydimethylsiloxane (PDMS) and a glass sphere (along with a number of controls) was investigated using indentation. Experiments were analyzed to quantify adhesion by estimating the energy release rate (ERR) and in terms of the maximum pull-off force for various pairings. Polyelectrolyte-treated pairings had toughness two to three times in excess of the controls, and a maximum pull-off force approximately 12 times that of the controls. Although attraction between opposite charges clearly drives the multilayer deposition, it was found that after two opposing surfaces have been brought into contact, adhesion was highest for surfaces with PAA, i.e. like-charges, on both sides.

1. Introduction:

Polyelectrolyte layer-by-layer deposition consists of adsorbing alternating layers of polyanions and polycations to a surface.[1] This is accomplished, for example, by placing a negatively charged surface in a polycation solution during which process the polycation adsorbs onto the surface, rendering it positively charged. The substrate is then moved into a polyanion solution where it acquires a negative surface charge upon adsorption. This process is repeated to place additional layers on the surface.

This method can be used to fabricate photo-active surfaces, electro- or photo-chromatic devices, solar cells, semiconductor devices, and to modify the hydrophobic/hydrophilic character of a surface. In biochemical applications, these layer-by-layer polyelectrolyte structures can be used in gas filtration, free radical trapping, controlled DNA delivery, pH-sensitive gated porous capsules or films, and can be used to build biological reactors.[2] Polyelectrolyte deposition in this fashion can also be used to inhibit bacterial growth, support mammalian cellular growth, or engineer tissues.[3,4]

Polyelectrolyte multilayers are assembled by taking advantage of their adhesive qualities, and their potential to encounter mechanical loads or other polyelectrolyte-treated surfaces in use makes their mechanical behavior and interaction crucial to function. Additionally, understanding relationships between the cohesive and adhesive nature of polyelectrolyte multilayers and their structure may help develop additional uses for polyelectrolyte treatments, such as for use in creating selectively adhesive surfaces.[5,6]

Mechanical tests using indentation have previously been performed on these types of polyelectrolyte layers. However the focus of these tests has been on the determination of Young's modulus of the polyelectrolyte films themselves. Moreover, tests are often performed on free-standing films rather than on films serving as surface treatments to modify properties of other substrates.[3,4,7-11] Observations about adhesion based on these studies are usually qualitative or semi-quantitative. The studies typically utilize micron-scale glass spheres

attached to atomic force microscope (AFM) cantilevers, either coated in polyelectrolytes themselves or simply cleaned using oxygen plasma.[12]

Macroscopic mechanical tests have been performed on polyelectrolyte layers, including shear tests[13,14] and "zero motion" tests with treated surfaces being placed together and pulled apart slowly enough to approximate the absence of kinetic effects.[15] It appears that material transfer does often occur, with contact, yielding differing results upon repeated contacts in the same location. The bulk of these studies were conducted in air, with relatively little focus on aqueous environmental effects, as would be the case in most biological applications.

Here, we report on a study of adhesion in an aqueous environment between polyelectrolyte multilayers using indentation by a rigid sphere of an elastomeric substrate, with each side of the interface optionally coated by polyelectrolyte layers. Raw force-deflection data are analyzed to extract interfacial toughness and maximum tensile load sustained by the contact.

2. Experimental Methods:

2.1. Materials Selection:

Much work has been reported on surface modification through polyelectrolyte deposition using polydimethylsiloxane (PDMS), glass, and silicon as substrates. Several methods for attaching charges to the surface of these structures have been well explored.[16,17,18] For the purposes of this work, PDMS and glass were favored over silicon as it is necessary to use at least a single compliant surface, and oxygen-plasma cleaned PDMS and glass can be treated using the same methods in order to apply polyelectrolyte surface layers.

While it is necessary that one of the two surfaces be compliant in order to study adhesion energy by means of change in contact area, it is convenient for the other to be relatively rigid. (See 2.3. Measurement of Adhesion:, page 6.) For this reason, one PDMS surface and one glass surface were used.

The PDMS utilized in this experiment was Sylgard ® 184 Silicone Elastomer Kit using 10 wt% curing agent. The PDMS films were 0.78 mm thick. Indenters were produced from soda-lime glass rods with a nominal radius of 1.0 mm, held and rotated by hand under a propane flame until a desired tip radius of approximately 2.10 mm was reached. Polyelectrolytes were chosen based on previous studies[19] and availability of molecular weights. Poly(acrylic acid) 25% solution in water (PAA) (average Mw = 50,000), purchased from Polysciences Inc., and poly(allylamine hydrochloride) (PAH) (average Mw = 58,000), purchased from Sigma-Aldrich, were used.

2.2 Surface Modification:

Polyelectrolyte layers, while not covalently bound to each other or to the substrate, can be produced in minutes using no more than a phosphate or sodium chloride buffer, [19,20] and the constituent polyelectrolytes are safe enough to be used in diapers.[21] Both PDMS and glass can be modified by oxygen-plasma treatment to form hydroxyl groups on their surfaces.[18] In an aqueous environment, these groups function as a negative charge modification. This treatment was used as a control for surfaces that had been modified with polyelectrolytes. The polyelectrolytes used in these experiments were poly(acrylic acid) (PAA) and poly(allylamine hydrochloride) (PAH). The two were deposited according to the method published by Elzbieciak et al.[19] The details of the procedures used to activate and treat surfaces in these experiments can be found in the supporting information. The various forms of surface treatment used in this series of experiments can be seen below in Figure 1 as measured by AFM.

It can be observed here, as well as in other studies,[19] that the adsorbed polyelectrolyte multilayers do not form smooth, flat surface coatings. In polyelectrolyte-treated surfaces, an obvious pattern of peaks and valleys can be observed.

The multilayers were added by submerging PDMS or glass into baths of 0.5 g/l polyelectrolyte under “strongly charged” conditions (pH = 3.0 for PAH, 11.0 for PAA) as outlined by Elzbieciak et al.[19] Multilayers prepared for these experiments were terminated at 5 or 6

layers (PAH or PAA, respectively). After oxygen plasma treatment, the first layer deposited was always PAH, followed by PAA, followed by PAH again and so on. The surface treatments thus resulted in multilayers of the form $(PAH\text{-}PAA)_X$-PAH or $(PAH\text{-}PAA)_X$, abbreviated PAH(2x+1) and PAA(2x) (in these cases, PAH(5) & PAA(6) representing $(PAH\text{-}PAA)_2$-PAH or $(PAH\text{-}PAA)_X$ and $(PAH\text{-}PAA)_3$, respectively). Each layer was deposited with a ten-minute submergence in the electrolyte solution, then rinsed three times for two minutes in de-ionized water before having another layer added to the surface.

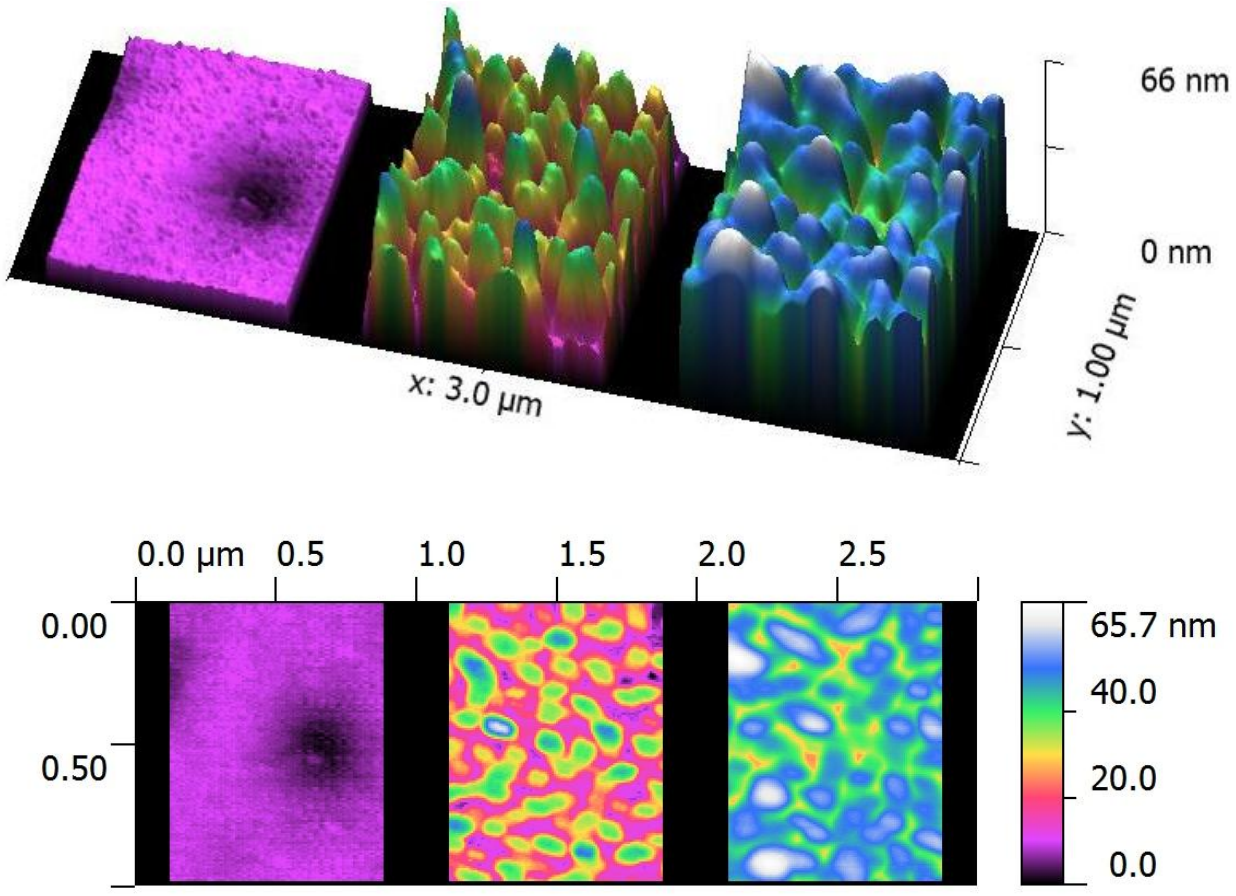

Figure 1: Surface treated PDMS shown in shared z-scale. Left to right: bare oxygen plasma-treated PDMS substrate, PAH(5), PAA(6).

2.3. Measurement of Adhesion:

Adhesion was measured by means of indentation: a glass sphere (radius = 2.10 ± 0.07 mm) attached to a motor was brought into contact with a treated PDMS substrate (thickness = 0.78 ± 0.005 mm, indentation velocity = 0.001 mm/s, maximum depth of indentation = 0.03 mm), causing slight deformation as the sphere pressed into the surface. The sphere was then retracted from the surface at the same speed. These tests were performed in a phosphate buffered saline (PBS) medium, with a pH set to 7.4 to simulate in-vivo conditions[22]. An inverted microscope beneath the apparatus observed the area of contact, and a capacitance displacement sensor was used to determine the depth of penetration into the substrate. A force gauge placed in-line between the glass sphere and motor monitored the force applied by the indenter to the PDMS substrate during this process. The area of contact was continually monitored. This apparatus is represented schematically below in Figure 2.

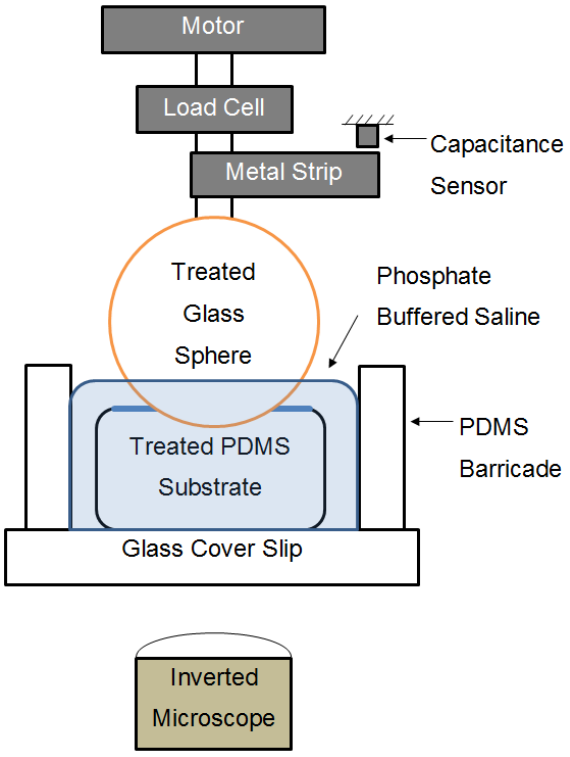

Figure 2: Indentation setup schematic.

Displacement of the glass indenter and the force exerted thereupon (Figure 3) are measured. The associated area of contact is observed through the microscope over which the test is performed. Using these three pieces of information and previously developed methods,[23] the associated energy release rate of contact can be calculated using a model-independent method. The technique reported by Vajpayee et. al.[23] was modified as follows.

Data from pairs of surfaces modified by polyelectrolytes (red, Figure 3, below) is compared to data from a "zero-adhesion control case, wherein hysteresis and maximum pull-off force are minimal (black, Figure 3, below). To calculate the strain energy requires knowledge of the loading path, absent adhesion, which has been previously termed the "Hertz curve". It is assumed that the adhesion upon indentation and prior to retraction is negligible.

For the entire process of indentation and retraction, the energy deficit is the whole of the area enclosed by the force-displacement indentation and retraction curves. The ERR is the rate of change in this deficit with respect to area of contact. To match areas of contact to known ERR values, energy deficit values must be found for a series of areas of contact.

The area of contact will be greatest at the deepest point of indentation. For all other depths, there will be points on both the indenting and retracting force-depth curves that share equal areas of contact. These pairs of points must be found, matched, and assigned an energy deficit value.

Equal areas of contact also share a single compliance value. Thus, to find the point 'O' on the retracting curve with area of contact equal to that of the indenting curve, a tangent line is drawn to the retracting line from a point 'O_H' on the indenting curve. An example tangent line can be seen below in Figure 3, and the corresponding mathematical term provided in Equation 1.

$$Energy\ Deficit = \int_{O}^{O_H} F_{tan}\,d\delta + \int_{O_H}^{\delta max} F_{indent}\,d\delta - \int_{O}^{\delta max} F_{retract}\,d\delta \quad (1)$$

where F is force of a particular curve, δ displacement (δ > 0 representing indentation into the substrate, δ < 0 representing retraction from the nominal surface), and δ_{max} the displacement at greatest indentation into the substrate.

Areas of contact for 'O_H' points along the indenting curve (and therefore also for the associated 'O' points) were calculated using the theoretical area of contact of Hertzian non-adhesive elastic contact.[24] The equations used are reproduced below in Equations 2 and 3.

These values were confirmed with measurements of area of contact from still images taken from the microscope viewing the experiment.

$$\delta' = \delta\left(0.4 + 0.6\exp\left(\frac{-1.8a}{h}\right)\right) \tag{2}$$

Rearranging and substituting to solve iteratively for *A*,

$$0.4 + 0.6\exp\left(-1.8\sqrt{\frac{A}{\pi}}/h\right)A = \pi \cdot r \cdot \delta'$$

$$A_{i+1} = \frac{\pi \cdot r \cdot \delta'}{0.4 + 0.6\exp\left(\dfrac{-1.8\sqrt{\dfrac{A_i}{\pi}}}{h}\right)} \tag{3}$$

where δ is the depth of penetration into the substrate for an infinitely thick substrate (equal to a^2/R), δ' is the corrected depth of penetration into the substrate, *a* is the radius of the area of contact, *h* is the substrate thickness, and *A* is the area of contact. The latter calculation is repeated until the difference between A_{i+1} and A_i is less than one percent.

The energy lost between these two points O_H and O is the area of the enclosed region of the indenting curve, the retracting curve, and this tangent line. This was calculated numerically for sets of experimental data. If there is little hysteresis between indentation and retraction, the loss of energy between the two stages is small, as in the dashed data set, oxygen plasma on

oxygen plasma, Figure 3A, below. If, however, the hysteresis is large, the loss of energy is correspondingly great, as in the solid data set, PAA(6) on PAA(6), Figure 3A. The energy deficit calculated for a specified O-O_H point pairing and the associated area over a series of such sets of points can be used to calculate the energy deficit as a function of area. The derivative of this relationship is the ERR for a given pairing of surfaces. These relationships are derived for the example data in Figure 3A below in Figure 3B. The low adhesion dashed plot represent an oxygen plasma-oxygen plasma control set and the adhesive solid plot represent a PAA(6)-PAA(6) pairing.

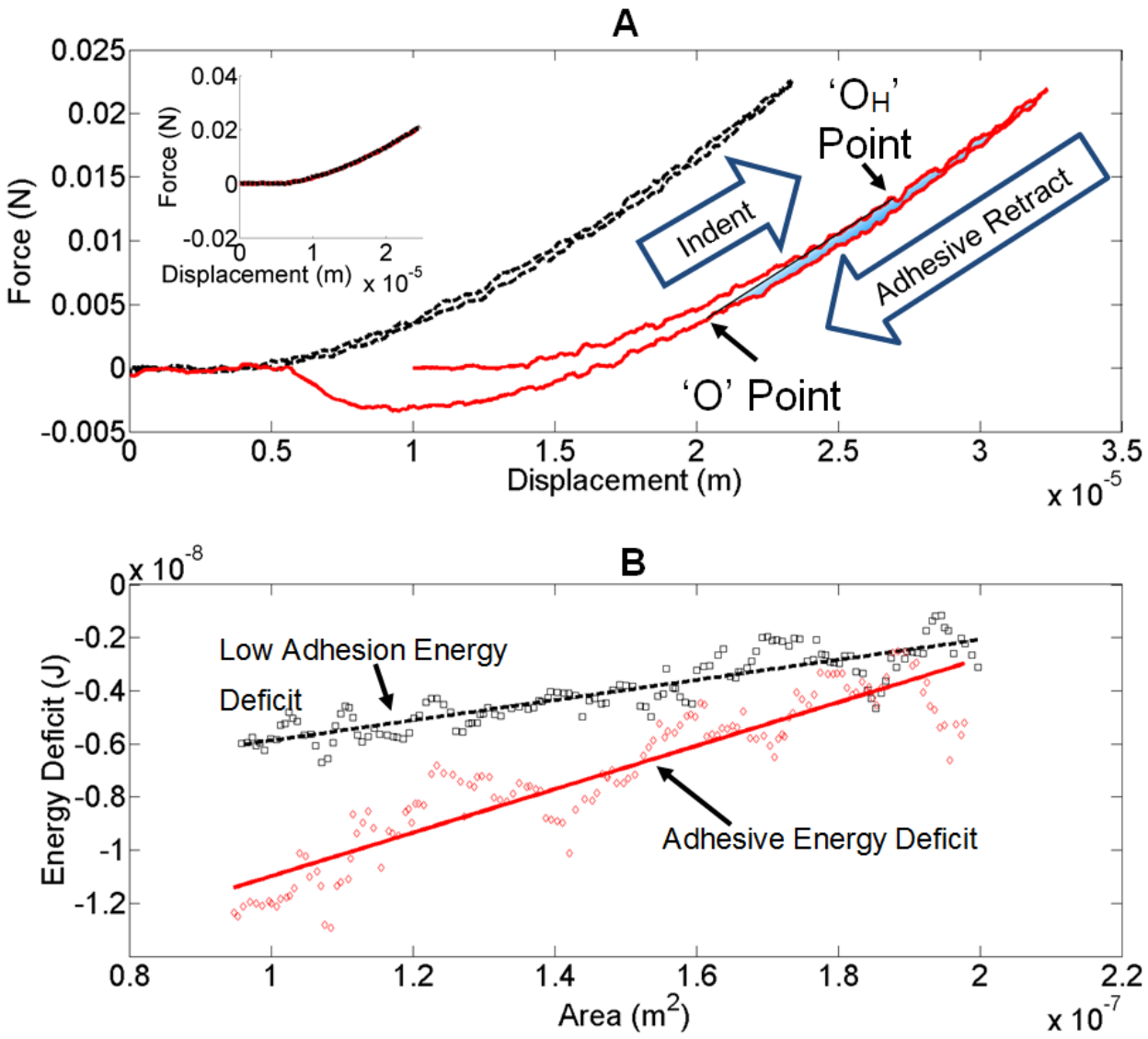

Figure 3: (A) Low hysteresis, low energy loss indentation typical of oxygen plasma-treated glass indenter and PDMS substrate (dashed) and high hysteresis, high energy loss indentation from PAA(6) treated glass indenter against PAA(6) treated PDMS (solid, shown shifted right). Observe similarity of indentation curves. A single paired set of O and OH points and the associate energy deficit (shaded region) are shown. Note adhesion indicated by negative force, or pull-off force, at negative depth of indentation (indicating a point above the surface). (B) Corresponding calculated energy deficit values and linear slopes. (A, Inset) Overlaid indentation data for the two cases are nearly identical, showing that there is little influence of adhesion in either case.

Observation of the influence of surface treatment on resulting energy release rates, and thus losses due to adhesion, provides a quantitative tool for the comparison of adhesion between different systems.

Energy release rates (ERR) and maximum pull-off force (MPO) values were measured for five repeated indentations at the same location on the substrate. The hypothesis that the mean slope of these curves was zero was tested. The average slope for ERR was found to be -0.000710 Jm^{-2}/indent, with a standard deviation of 0.000402 Jm^{-2}/indent. At 95% confidence, this results in possible slopes ranging from +0.000079 to -0.001498 Jm^{-2}/indent. For MPO values, the average slope was found to be -4.138×10^{-7} N/indent with a standard deviation of 3.619×10^{-6} N/indent. At 95% confidence, the possible range of slopes for these data are $+6.679 \times 10^{-6}$ to -7.507×10^{-6}. Because both of these ranges cross zero, the null hypothesis is accepted. See supporting information for data used in these calculations. These trends are shown below in Figure 4.

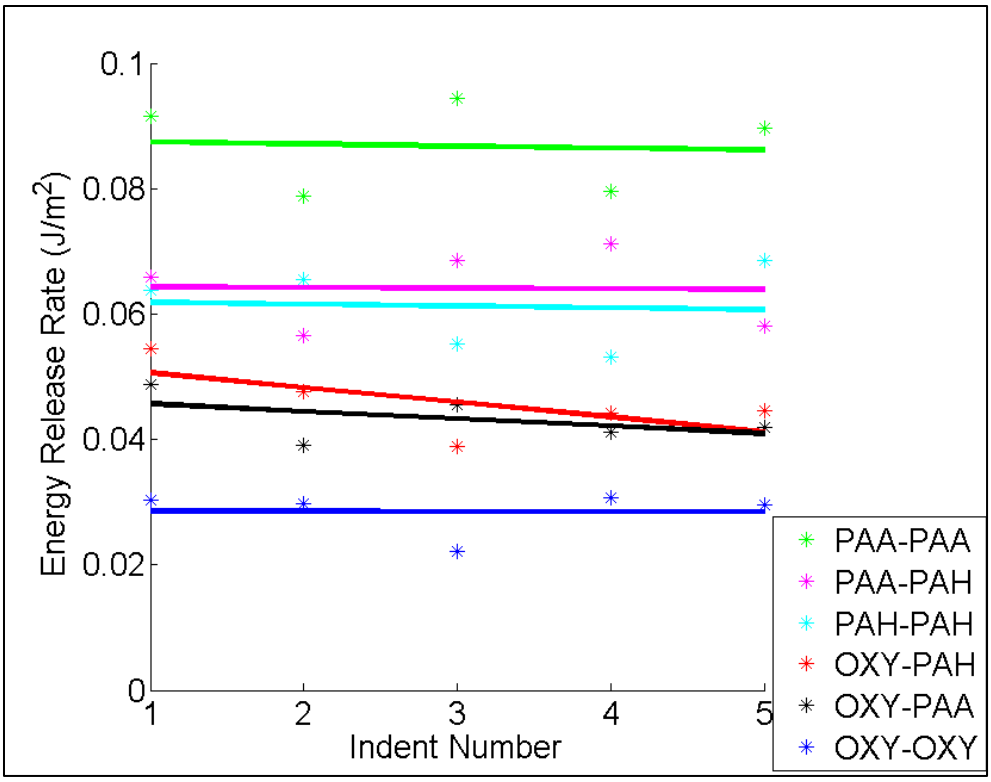

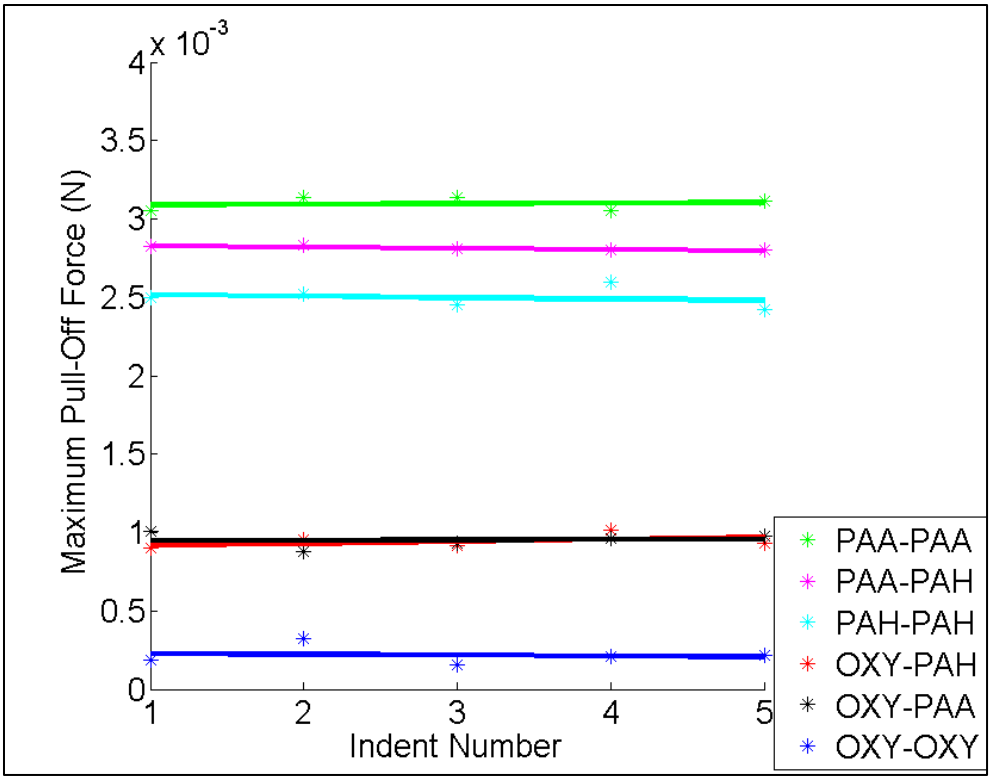

Figure 4: Stability of extracted interfacial properties over tested ranges.

Based on the hypothesis test, the results and discussion of this work assumes that there is no significant difference between indentations one through five.

3. Results:

ERR and maximum pull-off force (MPO) values for pairings of polyelectrolyte treated surfaces are in excess of pairings of control surfaces, regardless of the pair of polyelectrolytes in question. ERR and MPO values for pairings of oxygen-plasma control surfaces with polyelectrolyte treated surfaces fell somewhere between the two (Figure 5).

These data can be corrected to treat all energy loss during oxygen plasma to oxygen plasma contacts as bulk energy dissipation by subtracting the oxygen plasma-oxygen plasma ERR value from all ERR values. This results in a corrected Energy Release Rate (cERR) based on the oxygen plasma control.

Assuming a system of surfaces terminated with one of two surface treatments, A and B, three possible combinations of surface contact are possible: A-A, A-B, and B-B. Assuming

there is significant differentiation between the adhesive strength of these three combinations, adhesion between the surfaces in the system will be selectively adhesive. The cERR and MPO values shown in Figure 5 are reorganized into possible combinations of these two-type systems below in Figure 6. These data show that a system of PAA and PAH-terminated surfaces will show relatively little selectivity with all surfaces adhering on contact, while a system of PAA and oxygen plasma-terminated surfaces will result in strong adhesion between PAA-terminated surfaces, weaker adhesion between PAA and oxygen plasma-terminated surfaces, and effectively no adhesion between pairs of oxygen plasma-terminated surfaces.

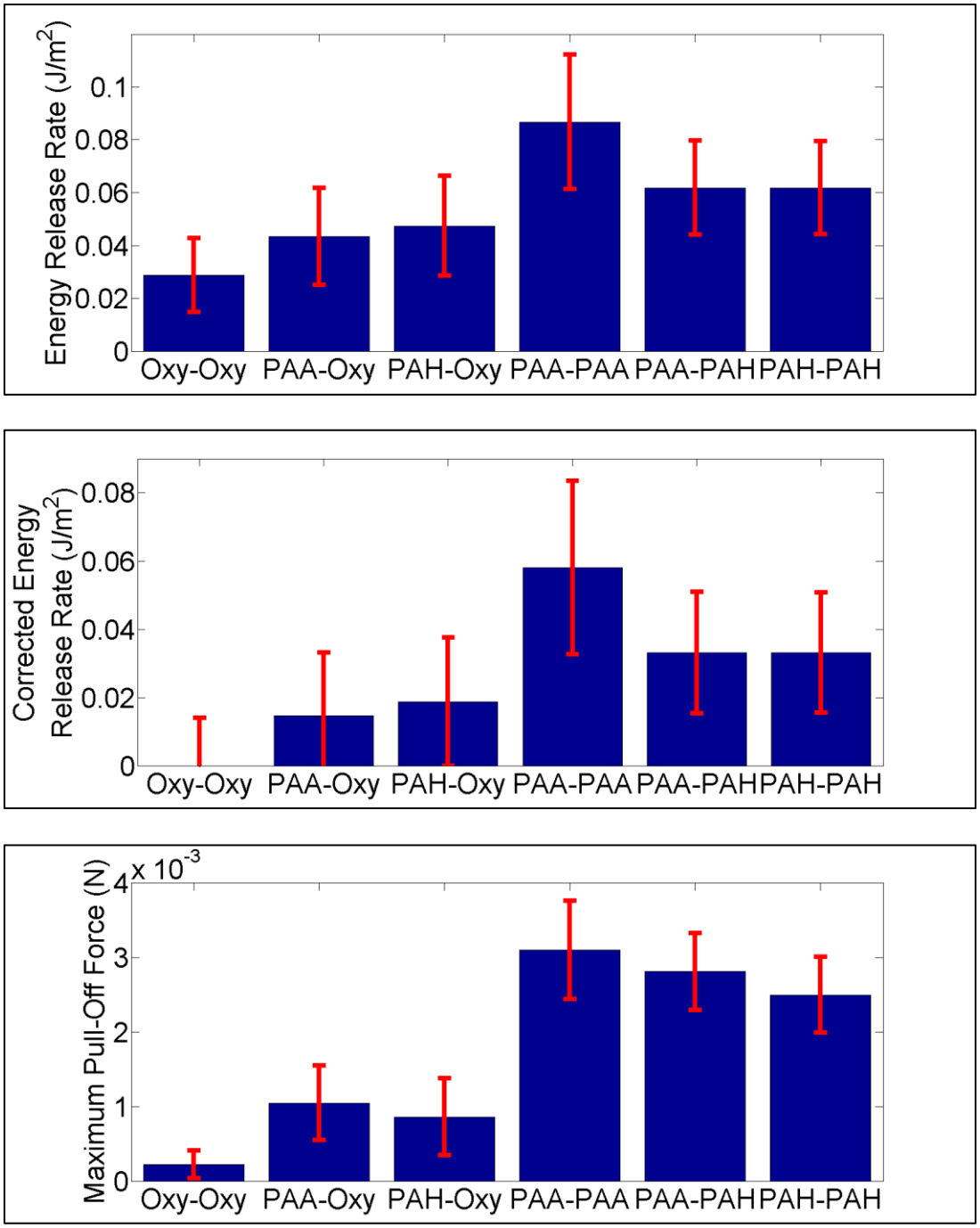

Figure 5: ERR, corrected ERR (cERR), and MPO over first five indentations into surface sorted by pairing. Note consistency of trends between ERR and MPO measurements. Standard deviation of measurements shown in error bars.

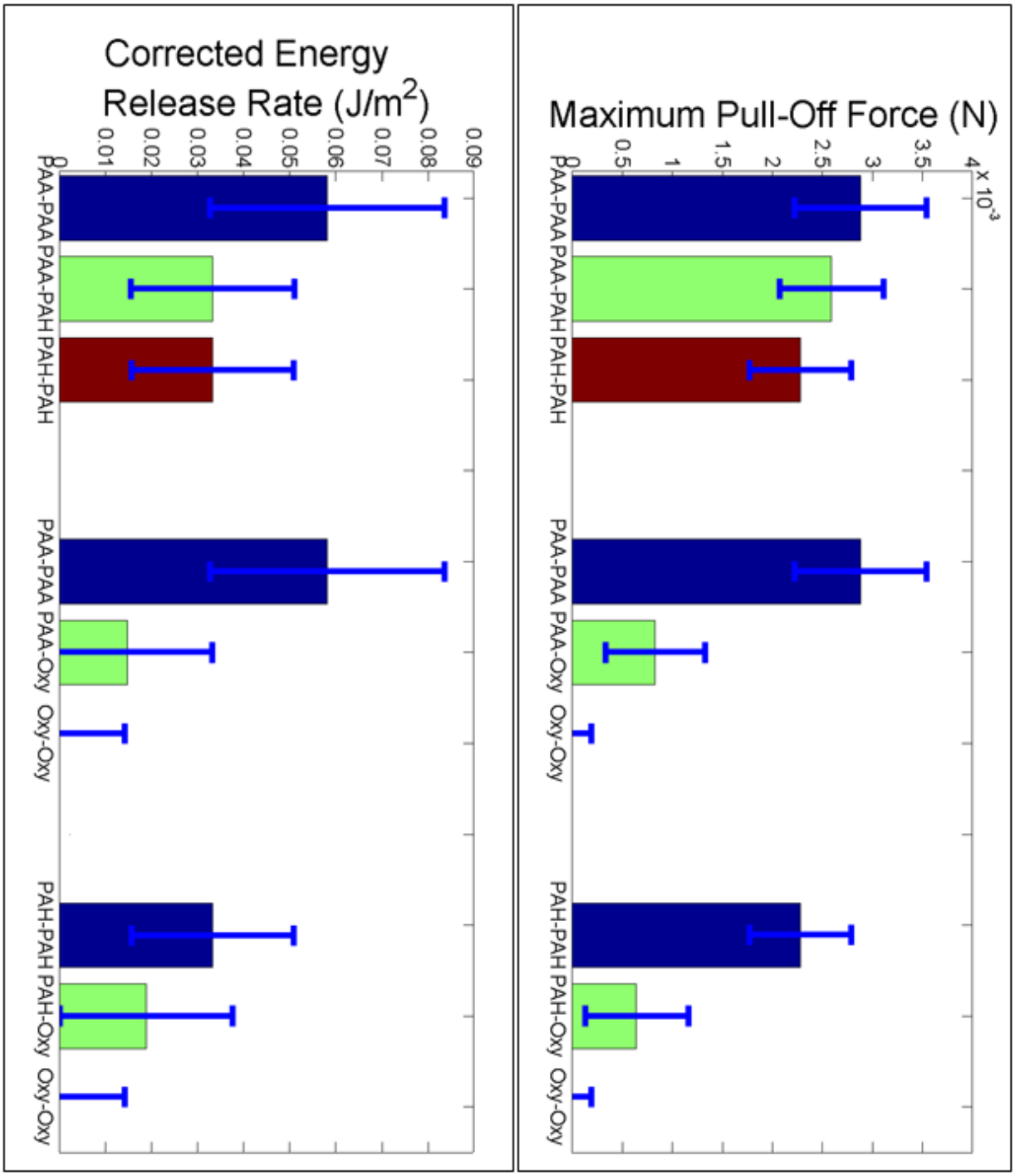

Figure 6: Surface interactions between different possible pairings in various two-surface systems. Note various degrees of selectivity in systems combining one polyelectrolyte treated surface and one oxygen-plasma treated surface.

4. Conclusions:

These data suggest that, counter to expectation, polyelectrolyte-treated surfaces adhere regardless of the charge-group of their terminally-adsorbed layer. It is clear that before contact the amine groups present in PAH attract the hydroxyl groups present on PAA or on oxygen-plasma treated surfaces; this attraction is used to assemble the multilayered suface. However, our experiments show that forces resisting separation after contact are attractive between all polyelectrolyte sufaces, with a significantly reduced attraction to oxygen-plasma treated surfaces. This could be explained by the structures formed atop polyelectrolyte treated surfaces, which continue to grow with additional adsorption of layers but do not appear to fully merge (see Figure 7 and Figure 8, below).

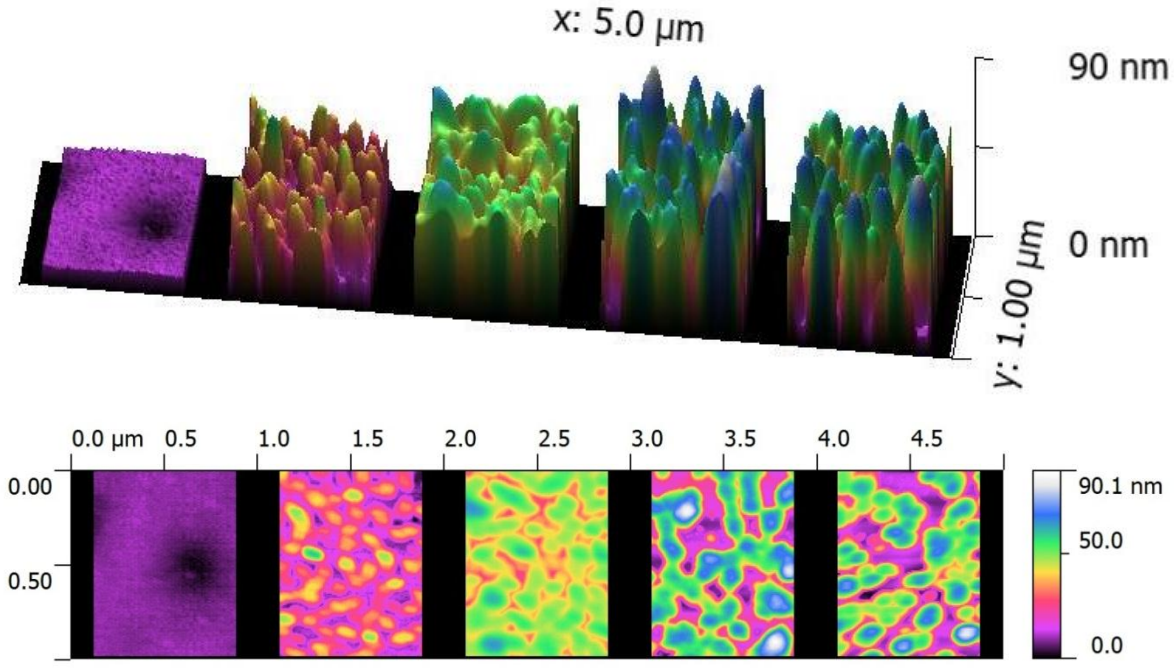

Figure 7: Isometric and top-down example views of surface structures of differently-treated surfaces. Left to right: bare oxygen plasma-treated PDMS substrate, PAH(5), PAA(6), PAH(13), PAA(14). Note relatively constant diameter of finger-like surface extensions regardless of number of deposited surface layers.

While early experiments in selective surface treatment showed these surface profiles do not reach all the way to the substrate at their bases and be form fully merged structures lower

down (see supporting information), there are ever-present a series of similarly sized and spaced finger-like extensions off of the surface of the substrate. It appears likely that it is the interaction of these uppermost structures that causes strong adhesion regardless of terminal surface treatment.

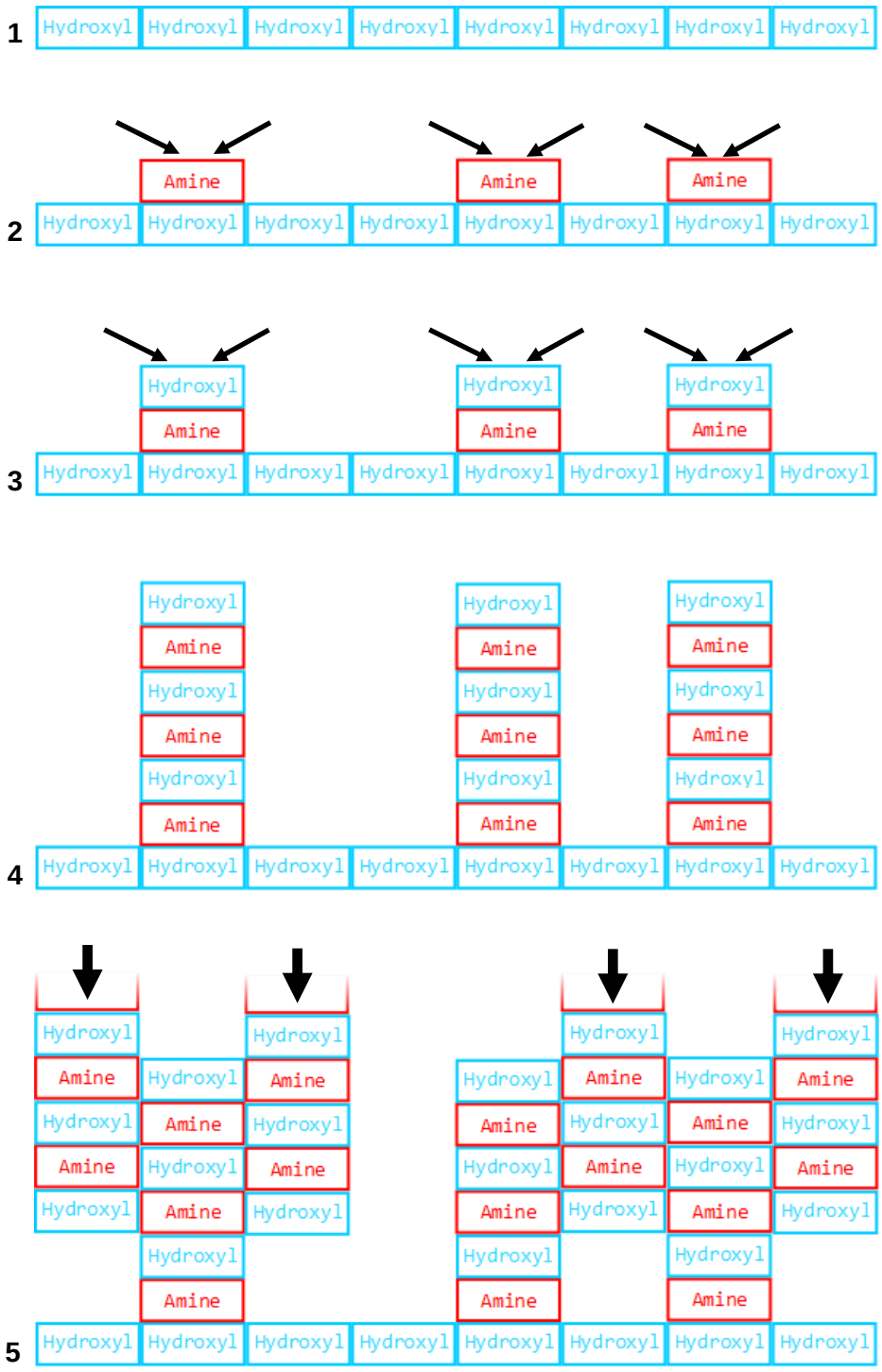

Figure 8: Schematic of hypothesized development and interaction of polyelectrolyte structures in two dimensions (not to scale). 1: Oxygen plasma-treated PDMS develops hydroxyl groups. 2: PAH adheres to surface in some areas forming amine-rich zones. 3. PAA adheres to PAH areas. 4. Process of adsorption continues to form multilayers. 5. Multilayers from another treated structure are encountered.

Through the course of this study, a method of indentation has been developed to quantify adhesion and compare changes to adhesion resulting from polyelectrolyte surface treatments to a compliant substrate. Except for energy losses attributed to bulk deformation of the substrate, repulsive controls appear to have small adhesion compared to pairings of treated surfaces. This method of examination can be used to study the influence of differing conditions of surface deposition, such as varying polyelectrolyte solution pH or number of adsorbed layers, or between differing conditions of indentation, such as variations in salt concentration.

6. References:

1. Decher, *Science*, Fuzzy Nanoassemblies: Toward Layered Polymeric Multicomposites, (1997), Pp. 1232-1237
2. Ariga, *Physical chemistry chemical physics*, Layer-by-layer assembly as a versatile bottom-up nanofabrication technique for exploratory research and realistic application, (2007), p 2319.
3. Gribova, *Chemistry of Materials*, Polyelectrolyte Multilayer Assemblies on Materials Surfaces: From Cell Adhesion to Tissue Engineering, (2011), Article ASAP.
4. Tang, Z., Wang, Y., Podsiadlo, P. and Kotov, N, *Advanced Materials*, Biomedical Applications of Layer-by-Layer Assembly: From Biomimetics to Tissue Engineering, (2006), Pp 3203–3224.
5. Bai, Jin, Jagota, Hui, *Journal of Applied Physics*, Adhesion selectivity by electrostatic complementarity I One-dimensional stripes of charge, 110, 054902, (2011).
6. Bai, Jin, Jagota, Hui, *Journal of Applied Physics*, Adhesion selectivity by electrostatic complementarity I Two-dimensional analysis, 110, 054903, (2011).
7. Elzbieciak, Langmuir, Influence of pH on the Structure of Multilayer Films Composed of Strong and Weak Polyelectrolytes, (2009), Pp 3255–3259.
8. Mermut, *Macromolecules*, Structural and Mechanical Properties of Polyelectrolyte Multilayer Films Studied by AFM, (2003), Pp.8819-8824.
9. Gong, *Langmuir*, Interaction and Adhesion Properties of Polyelectrolyte Multilayers, (2005), Pp.7545-7550.
10. Picart, *Colloids and Surfaces*, Measuring mechanical properties of polyelectrolyte multilayer thin films: Novel methods based on AFM and optical techniques, (2007), Pp.30-36.
11. Bosio, *Colloids and Surfaces*, Interactions between silica surfaces coated by polyelectrolyte multilayers in aqueous environment: comparison between precursor and multilayer regime, (2004), Pp.147-155.
12. V. Bosio et al., *Colloids and Surfaces A: Physicochem*, Interactions between silica surfaces coated by polyelectrolyte, (2004) Pp.147–155.
13. Matsukuma, *Langmuir*, Adhesion of Two Physically Contacting Planar Substrates Coated with Layer-by-Layer Assembled Films, (2009), Pp. 9824–9830.
14. Zhou, *BioResources*, Layer-by-layer Nanoscale Bondlines for Macroscale adhesion, (2010), Pp. 1530-1541.
15. Claesson, *Advances in Colloid and Interface Science*, Polyelectrolytes as adhesion modifiers, (2003), Pp. 53-74.
16. Chaudhury, Whitesides, *Science,* Correlation between surface free energy and surface constitution, (1992), Vol: 255, 5049 Pp. 1230-1232.
17. Sharp Et Al, *Langmuir,* Effect of Stamp Deformation on the Quality of Microcontact Printing Theory and Experiment, (2004), 20, Pp. 6430-6438.
18. Chaudhury, Whitesides, *Langmuir,* Direct Measurement of Interfacial Interactions between Semispherical Lenses and Flat Sheets of Poly(dimethylsiloxane) and Their Chemical Derivatives, (1991), 7, Pp. 1013-1025.
19. Elzbieciak, *Colloids and Surfaces A: Physicochemical and Engineering Aspects*, Nonlinear growth of multilayer films formed from weak polyelectrolytes, (2009), 343, 89-95.
20. Zimmermann Et Al, *Langmuir,* Electrokinetic Characterization of Poly(Acrylic Acid) and Poly(Ethylene Oxide) Brushes in Aqueous Electrolyte Solutions, (2005), 21, Pp. 5108-5114.
21. Elliott, *Polymer,* Structure and swelling of poly(acrylic acid) hydrogels effect of pH, ionic strength, and dilution on the crosslinked polymer structure, (2004), Vol: 45, 5, Pp. 1503-1510.
22. Vivian McAlister, Karen E. A. Burns, Tammy Znajda, and Brian Church. "Hypertonic Saline for Peri-operative Fluid Management" Cochrane Database of Systematic Reviews.1 (2010).

23. Vajpayee, *Langmuir,* Model-Independent Extraction of Adhesion Energy from Indentation Experiments, (2008), 24, Pp. 9401-9409.
24. Shull, *Materials Science and Engineering R*, Contact Mechanics and the Adhesion of Soft Solids,(2002) 36, Pp. 1–45

7. Supporting Information:

7.1 Testing Accuracy of Method Used to Calculate Energy Deficit

The program used to calculate energy deficit values from a given set of data points was tested using a hypothetical data set with a predictable result. It was first tested with a simple, linear data set, then with the hypothetical and more realistic hyperbolic data set presented below. Error was found to be less than 5% in either case.

O_H point ≡ a point on the indenting curve for which a corresponding point O on the retracting curve with the same area and calculable energy deficit exists.

Since area of contact determines the compliance of the substrate, lines of constant compliance connect O_H to O. These lines are tangent to the indenting curve at their respective O_H points.

Tangent line ≡ the line tangent to the indenting curve at O_H.

The O point of an O_H is the minimum intersection of the tangent line with the retracting curve.

$$O(O_H) \equiv \min\left(tangent\ line \cap indent\ curve\right) \tag{4}$$

Deficit, as defined in equation 1,

$$Energy\ Deficit = \int_O^{O_H} F_{tan}\,d\delta + \int_{O_H}^{\delta max} F_{indent}\,d\delta - \int_O^{\delta max} F_{retract}\,d\delta \tag{5}$$

Each of these lines is highly visible in the below diagram (a depiction of the test data used in this supporting information).

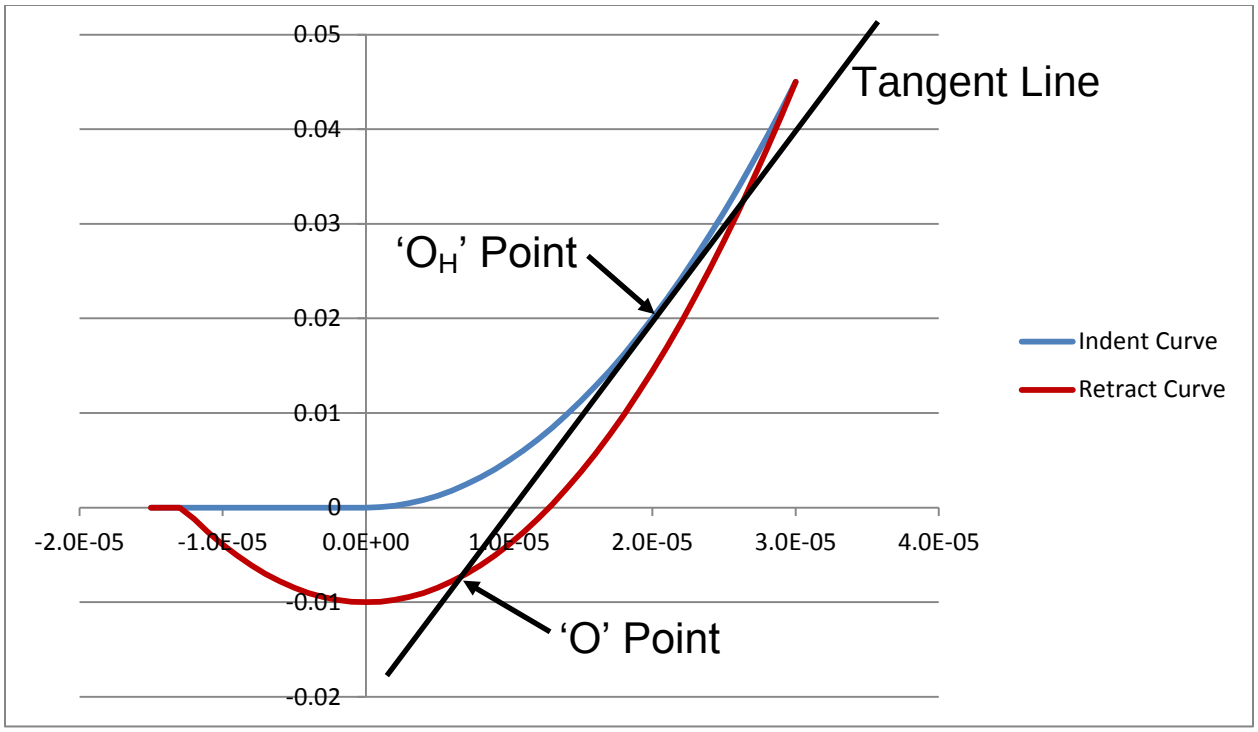

Figure A1: Simulated indentation curve.

Now entering synthetic data set calculations

$$indent\ curve \equiv F_{indent} = c_1\delta^2 \tag{6}$$

$$retract\ curve \equiv F_{retract} = \left(c_2\delta^2\right) - c_3 \tag{7}$$

$$\frac{d}{d\delta}F_{indent} = 2c_1\delta \tag{8}$$

Point slope equation of a line:

$$F - F_1 = m(\delta - \delta_1) \tag{9}$$

$$\delta_1 = OH\ \ point\ depth \tag{10}$$

$$m = \frac{d}{d\delta}F_{indent}(\delta_1) = 2c_1\delta_1 \tag{11}$$

$$F_1 = F_{indent}(\delta) = c_1\delta_1^2 \tag{12}$$

Substitute into point slope form:

$$F - c_1\delta_1^2 = 2c_1\delta_1(\delta - \delta_1) \tag{13}$$

$$F_{tan} = 2c_1\delta_1\delta - c_1\delta_1^2 \tag{14}$$

to find intersection with retract curve (O point):

$$F_{retract} = F_{tan} \tag{15}$$

$$F_{retract} = (c_2\delta^2) - c_3 \tag{16}$$

$$F_{tan} = 2c_1\delta_1\delta - c_1\delta_1^2 \tag{17}$$

$$(c_2\delta^2) - c_3 = 2c_1\delta_1\delta - c_1\delta_1^2 \tag{18}$$

$$(c_2)\delta^2 + (-2c_1\delta_1)\delta + (c_1\delta_1^2 - c_3) = 0 \tag{19}$$

Solve using quadratic equation

$$x = \frac{-b \pm \sqrt{b^2 - 4ac}}{2a} \tag{20}$$

$$O\ point\ is\ \min(intercept) \therefore x = \frac{-b - \sqrt{b^2 - 4ac}}{2a} \tag{21}$$

$$a = c_2 \tag{22}$$

$$b = -2c_1\delta_1 \tag{23}$$

$$c = c_1\delta_1^2 - c_3 \tag{24}$$

$$O(\delta_1) \equiv \frac{2c_1\delta_1 - \sqrt{4c_1^2\delta_1^2 - 4c_2(c_1\delta_1^2 - c_3)}}{2c_2} \tag{25}$$

Now using that to find the energy deficit

$$Energy\ Deficit = \left[\int_{O(\delta_1)}^{\delta_1} F_{tan}\, d\delta\right] + \left[\int_{\delta_1}^{\delta_{max}} F_{indent}\, d\delta\right] + \left[\int_{\delta_{max}}^{O(d_1)} F_{retract}\, d\delta\right] \tag{26}$$

$$Energy\ Deficit = \left[\int_{O(\delta_1)}^{\delta_1}\left(2c_1\delta_1\delta - c_1\delta_1^2\right)d\delta\right] + \left[\int_{\delta_1}^{\delta_{max}} c_1\delta^2\ d\delta\right] - \left[\int_{O(d_1)}^{\delta_{max}}\left(c_2\delta^2 - c_3\right)d\delta\right] \tag{27}$$

$$\int_{O(\delta_1)}^{\delta_1}\left(2c_1\delta_1\delta - c_1\delta_1^2\right)d\delta = \left(c_1\delta_1\delta^2 - c_1\delta_1^2\delta\right)\Big|_{O(\delta_1)}^{\delta_1} \tag{28}$$

$$\int_{\delta_1}^{\delta_{max}} c_1\delta^2\ d\delta = \frac{c_1\delta^3}{3}\Bigg|_{\delta_1}^{\delta_{max}} \tag{29}$$

$$\int_{O(d_1)}^{\delta_{max}}\left(c_2\delta^2 - c_3\right)d\delta = \left(\frac{c_2\delta^3}{3} - c_3\delta\right)\Bigg|_{O(\delta_1)}^{\delta_{max}} \tag{30}$$

$$Energy\ Deficit =$$

$$\left[\left(c_1\delta_1^3 - c_1\delta_1^3\right) - \left(c_1\delta_1 O(\delta_1)^2 - c_1\delta_1^2 O(\delta_1)\right)\right] + \left[\left(\frac{c_1\delta_{max}^3}{3}\right) - \left(\frac{c_1\delta_1^3}{3}\right)\right] - \left[\left(\frac{c_2\delta_{max}^3}{3} - c_3\delta_{max}\right) - \left(\frac{c_2 O(\delta_1)^3}{3} - c_3 O(\delta_1)\right)\right]$$

$$= c_1\delta_1 O(\delta_1)\left(\delta_1 - O(\delta_1)\right) + \frac{c_1}{3}\left(\delta_{max}^3 - \delta_1^3\right) + \frac{c_2}{3}\left(O(\delta_1)^3 - \delta_{max}^3\right) + c_3\left(\delta_{max} - O(\delta_1)\right)$$

$$O(\delta_1) \equiv \frac{2c_1\delta_1 - \sqrt{4c_1^2\delta_1^2 - 4c_2\left(c_1\delta_1^2 - c_3\right)}}{2c_2}$$

(31)

7.2 Statistical Analysis to Support Hypothesis that Adhesion Remains Unchanged Upon Repeated Indentation

Complete Fitting Parameters on Slope Values

Fitting Parameters: (Supporting Figure 4)

	PAA-PAH	PAA-PAA	PAH-PAH	0xy-PAH	0xy-PAA	0xy-0xy
Indent	ERR (J/m^2)					
1	0.06596	0.09159	0.06378	0.05444	0.04881	0.0303
2	0.05654	0.07879	0.06546	0.04769	0.03911	0.02967
3	0.06859	0.0943	0.05528	0.03886	0.0455	0.0222
4	0.07114	0.07961	0.0532	0.04414	0.04121	0.03077
5	0.05816	0.08958	0.0685	0.0445	0.04187	0.02957
Avg	0.06408	0.08677	0.06124	0.04592	0.0433	0.0285
Slope	-1E-04	-0.0003	-0.0003	-0.0023	-0.0012	-4E-05
	Slope Average	Slope Std	Slope Max	Slope Min		
	-0.0007	0.0004	7.9E-05	-0.0015		

	MP0 (N)					
Indent						
1	0.00282	0.00305	0.0025	0.0009	0.00101	0.00018
2	0.00283	0.00314	0.00252	0.00095	0.00088	0.00032
3	0.00281	0.00314	0.00245	0.00092	0.00093	0.00015
4	0.0028	0.00305	0.0026	0.00102	0.00096	0.00021
5	0.0028	0.00311	0.00242	0.00093	0.00098	0.00021
Avg	0.00281	0.0031	0.0025	0.00094	0.00095	0.00022
Slope	-8E-06	3.8E-06	-8E-06	1.3E-05	2.1E-06	-5E-06
	Slope Average	Slope Std	Slope Max	Slope Min		
	-4E-07	3.6E-06	6.7E-06	-8E-06		

Appendix 2: ERR & MPO values over multiple indentations and surface combinations showing fitting equations.

Column headers indicate the surface pairing whose data are shown in the below column. After data for the individual indents is shown, their average is calculated. The calculated slope and intercept for these measurements is calculated below. The standard error of each of these calculated slopes is given in the “Slope Err” row. The mean of the slopes calculated for all ERR and MPO values are shown in the first highlighted column and the standard deviations for these slopes in the second. The maximum and minimum slopes for a 95% confidence interval are shown in the third and fourth highlighted columns, respectively. Note that for both ERR and MPO calculations, these ranges cross zero.

7.3 Calculation for area of contacts

These calculations are used prior to their correction in accordance with equation 3.

$$\delta \equiv indenter\ \ depth$$

$$r \equiv radius\ of\ \ indenter$$

$$x \equiv radius\ of\ \ contact\ \ area$$

$$a^2 + b^2 = c^2 \tag{32}$$

$$x^2 + \left(r - \delta_1\right)^2 = r^2 \tag{33}$$

$$x^2 = r^2 - \left(r^2 - 2r\delta_1 + \delta_1^2\right) \tag{34}$$

$$A = 2r\delta_1 - \delta_1^2 \tag{35}$$

$$A = \pi R^2 \tag{36}$$

$$A = \pi\left(2r\delta_1 - \delta_1^2\right) \tag{37}$$

$$r - \delta_1\ \delta_1 \tag{38}$$

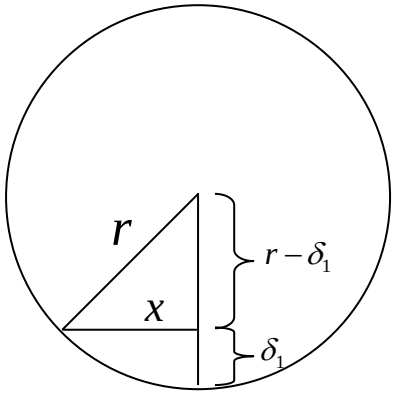

7.4 AFM Images of Surface Potential & Edges:

The following image sequence was taken using glass treated with PAH(13) deposited through micropipette dropping rather than dipping. The cutoff between the treated and untreated areas represents where a piece of PDMS was placed on the glass to allow for comparison after treatment. The PDMS was removed with forceps prior to imaging.

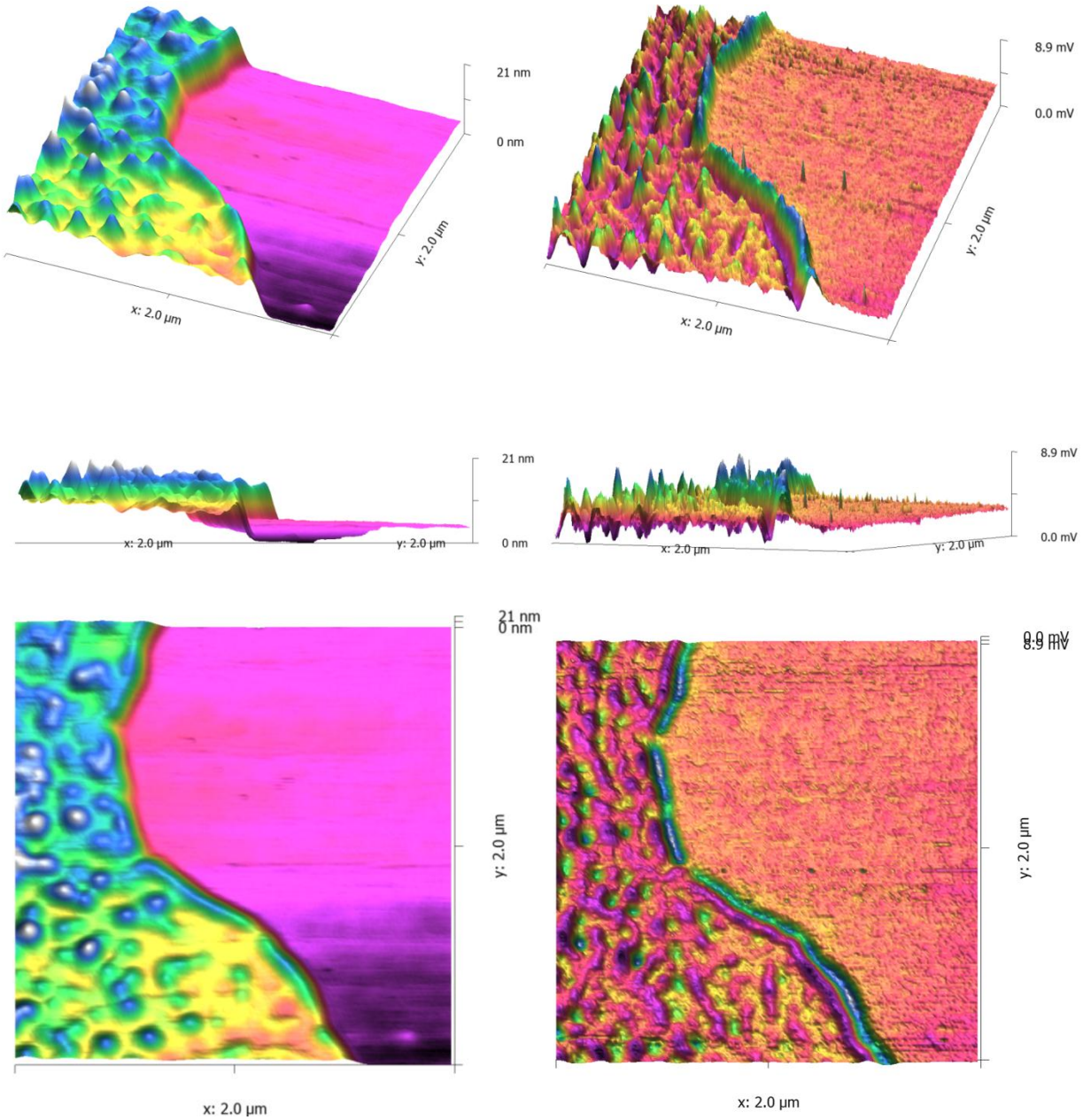

Figure A3: Isometric (top), side (middle), and top-down (bottom) 3D views of height (left) and charge map (right) of PAH(13) droplet-deposited on glass next to a protected area of glass for comparison.

7.5 Detailed Sample Preparation and Testing Procedure (Instrucional):

PDMS samples are mixed from Sylgard 184 Silicone Elastomer Kit at 10 wt% curing agent. The PDMS was degassed under vacuum until no bubbles were present, then cured at 80 °C for 2 hours between hydrophobic glass using 0.78 mm spacers. Glass indenters were prepared from Heat-Resistant Borosilicate glass purchased from McMaster-Carr, 2 mm diameter. Indenters were then melted to a diameter of approximately 4 mm by hand using a blowtorch. PDMS samples were pressed onto a glass slide. Indenters were inserted into a PDMS rack assembled on a glass slide.

Samples, glass or PDMS, were then placed in a Harrick plasma sterilizer/cleaner with attached Plasmaflo unit for pressure control. Pressure was reduced from atmospheric to 20 millitorr six times, then raised to 400 millitorr and held isobaric for 60s while the plasma chamber was set on HI RF and powered on.

Immediately from plasma cleaning, samples that were meant to be oxygen-plasma terminated were immersed in water. Samples meant to be polyelectrolyte terminated were immersed in PAH polyelectrolyte solution. Polyelectrolytes were purchased from Sigma Aldrich, PAH in dry salt form, PAA in liquid form. Polyelectrolyte solutions were created in accordance with Elzbieciak, at 0.50 g/l. PAH (poly(allylamine hydrochloride)) was mixed in pH 7.0 and pH 3.0 solutions. PAA (poly(acrylic acid)) was mixed in pH 7.0 and pH 11.0 solutions. Solvents were created from 0.15m NaCl solutions; pH was adjusted to desired value by adding NaOH or NaCl prior to the addition of polyelectrolyte. PAH was added 60 min prior to solution treatment to allow time for complete dissolution. PAA was added within a few minutes of treatment and mixed with a micropipette.

Polyelectrolytes were added to surfaces starting with PAH, then PAA, then PAH again and so on until the desired number of surface layers was reached. The first two bilayers (four individual monolayer treatments) were performed at pH 7.0. Subsequent layers were added at pH 3.0 or 11.0. Each layer was added by a 10-minute immersion in polyelectrolyte solution

followed by three separate immersions in deionized water for 2 minutes each. After the addition of the last surface layer, the samples were placed in deionized water until they could be tested.

Tests were performed on the mechanical setup in the lab depicted in Figure 2. The indenter was removed from the deionized water and a timer was started. Prior to reaching 5:00 minutes, the PDMS sample was placed beneath the indenter and surrounded by a PDMS barricade. The indenter was then lowered to just above the surface of the PDMS sample. At 5:00 minutes, PBS (phosphate buffered saline) was added to the surface of the PDMS sample forming a meniscus covering both surfaces. The program indentation_displ_10g.vi was run. The program was set for an indentation velocity = 0.001 of mm/s, maximum depth of indentation = 0.03 mm, 5 indentations. The program saves the information to a specified user-input filename and location, default Trial_1. After the conclusion of the indentation, the radius of the indenter must be measured precisely by digital caliper.

The filename and location must then be entered into the DefecitCalculatorIX.m program. It also assumes a file to be in the same location as Trial_1.lvm: Indenter.txt. This file should contain only the radius of the indenter used in the experiment measured in millimeters. The variable Check in DefecitCalculatorIX.m can be set to 1 to ascertain the degree of slip present in the test: this produces a mechanical data graph similar to that shown by indentation_displ_10g.vi using capacitor data instead of motor data. Setting this variable to 0 produces graphs for individual indentations and their associated ERR (energy release rate) data and prints the collected ERR values to the Matlab control screen. Setting it to 2 prints collected MPO (maximum pull-off forces) to the control screen.

8. Author Biography:

Walter A Jokiel was born September 29, 1987 in Pennsylvania to Richard and Elizabeth Jokiel. After graduating from Daniel Boone High School, Jokiel attended Lehigh University, obtaining Bachelor's degrees in Materials Science and Mechanical Engineering with high honors as an undergraduate student. Jokiel began his attachment to the Jagota Group as an undergraduate research assistant, working on the Group's Hybrids of Biological Molecules and Carbon Nanotubes Surfactant Exchange DNA-SWCNT project. Entering graduate studies, Jokiel remained with the Group, transitioning into the Biomimetic Architectures for Surface Mechanical Properties project area, developing this work on Charge Complementarity.